Gamow-Teller Interaction in the Decay of He^6†

B. M. RUSTAD AND S. L. RUBY*
Columbia University, New York, New York, and Brookhaven National Laboratory, Upton, New York
(Received November 9, 1954)

The coefficient α in the electron-neutrino angular correlation $W(\phi)=[1+\alpha(p/W)\cos\phi]$ for the He^6-Li^6 transition has been determined by measuring the coincidence rate between recoil ions and beta rays of selected energy as a function of the angle between the particles. Since the decay of He^6 (allowed ft value and $\Delta I=1$) obeys only Gamow-Teller selection rules, the interaction Hamiltonian for this transition is specified completely by $(G_A A+G_T T)$. The measured values of the correlation coefficient are $\alpha_{1.25}=+0.36\pm0.11$ for beta rays with mean energy 1.25 Mev and $\alpha_{2.0}=+0.31\pm0.14$ for the mean energy 2.0 Mev. These results are compared with $\alpha_T=+\frac{1}{3}$ and $\alpha_A=-\frac{1}{3}$ predicted from the pure tensor and axial vector invariants, respectively. The limiting value set by the experiment for (G_A/G_T) together with the observed absence of the Fierz interference terms for allowed beta spectra proves that the tensor invariant is dominant in the beta-decay interaction of He^6.

I. INTRODUCTION

THE study of the electron-neutrino (e-ν) angular correlations of allowed beta-active nuclei provides a method for identifying the Lorentz invariant operators of the beta-decay interaction Hamiltonian.[1] De Groot and Tolhoek[2] have calculated the allowed e-ν angular correlation for an arbitrary linear combination of the five independent invariants, which are customarily denoted by the letters S, T, V, A, and P. Their paper, as well as that by Hamilton,[3] emphasizes the fact that the angular correlations for different admixtures of the invariants differ in shape. Electron-recoil nucleus experiments to determine e-ν angular correlations have been reported in a number of papers.[4–6] Sherwin[4] measured the momenta of recoil nuclei from the decay of P^{32} which were detected in coincidence with beta rays emitted at specific angles with respect to the recoil ion beam. An approximately monolayer source of P^{32} was deposited on a thin composite film which had a sufficiently high work function to insure ionization for the S^{32} recoils. Although the majority of the recoil ions leaving the supporting surface were scattered, Sherwin was able to make the tentative conclusion that the e-ν angular correlation of P^{32} agreed approximately with the form $[1+(p/W)\cos\phi]$, where ϕ is the angle between the directions of emission of the particles and p and W are the relativistic momentum and energy of the electron. On the assumption that the transition must be parity forbidden (yes) to account for the large ft value, the results favor either the tensor or the axial vector invariant in the interaction Hamiltonian for the decay of P^{32}.

Allen *et al.*[5] used the beta-active gas, He^6, to eliminate any possible distortion of the recoil momentum spectrum that might arise from the inelastic scattering of recoil ions in escaping from a surface. The recoil nucleus spectra were measured by a repelling-grid technique. The statistical error in the data first reported was large because of the difficulties encountered in obtaining sufficient source definition and strength; however, the data could not be fitted to the angular correlations predicted from the scalar or the polar vector invariants. Recently, Allen and Jentschke[7] have published results, obtained with an improved apparatus, which suggest the angular correlation corresponding to the tensor interaction.

The problem of identifying the linear combination of the invariants from angular correlation measurements is made simpler and the results are less ambiguous if particular beta transitions are investigated for which selection rules may be used to restrict the number of possible linear combinations among the five invariant interactions. The He^6-Li^6 transition was chosen for the investigation reported in this paper because only the allowed selection rules ($\Delta I=1$, no) for the Gamow-Teller invariants (T and A) are obeyed. On the basis of the allowed ft value[8] of 815 ± 70 seconds and the nuclear spin change[9] $\Delta I=1$ for He^6, the selection rules that require $\Delta I=0$ are violated, and the nuclear matrix elements for the S, V, and P interactions vanish. The choice of He^6 is also favorable for experimental reasons. He^6 decays with the emission of a single electron and neutrino; the shape of the beta spectrum is of the simple allowed type[8] with an end-point energy of 3.50 ± 0.05 Mev. Since the gas is monatomic, there can be no distortion of the angular correlation between the electron and recoil nucleus from molecular binding effects. The charge and mass of the nucleus are small; and the

† Work performed under the research program of the U. S. Atomic Energy Commission.
* Present address; International Business Machine Corporation, Endicott, New York.
[1] F. Bloch and C. Møller, Nature **136**, 912 (1935).
[2] S. R. de Groot and H. A. Tolhoek, Physica **16**, 456 (1950).
[3] D. Hamilton, Phys. Rev. **71**, 456 (1947).
[4] C. W. Sherwin, Phys. Rev. **82**, 52 (1951); Phys. Rev. **73**, 216 (1948).
[5] Allen, Paneth, and Morrish, Phys. Rev. **75**, 570 (1949).
[6] O. Kofoed-Hansen and P. Kristensen, Phys. Rev. **82**, 96 (1951).
[7] J. S. Allen and W. K. Jentschke, Phys. Rev. **89**, 902 (1953).
[8] Wu, Rustad, Perez-Mendez, and Lidofsky, Phys. Revs. **87**, 1140 (1952).
[9] Hornyak, Lauritson, Morrison, and Fowler, Revs. Modern Phys. **22**, 291 (1950).

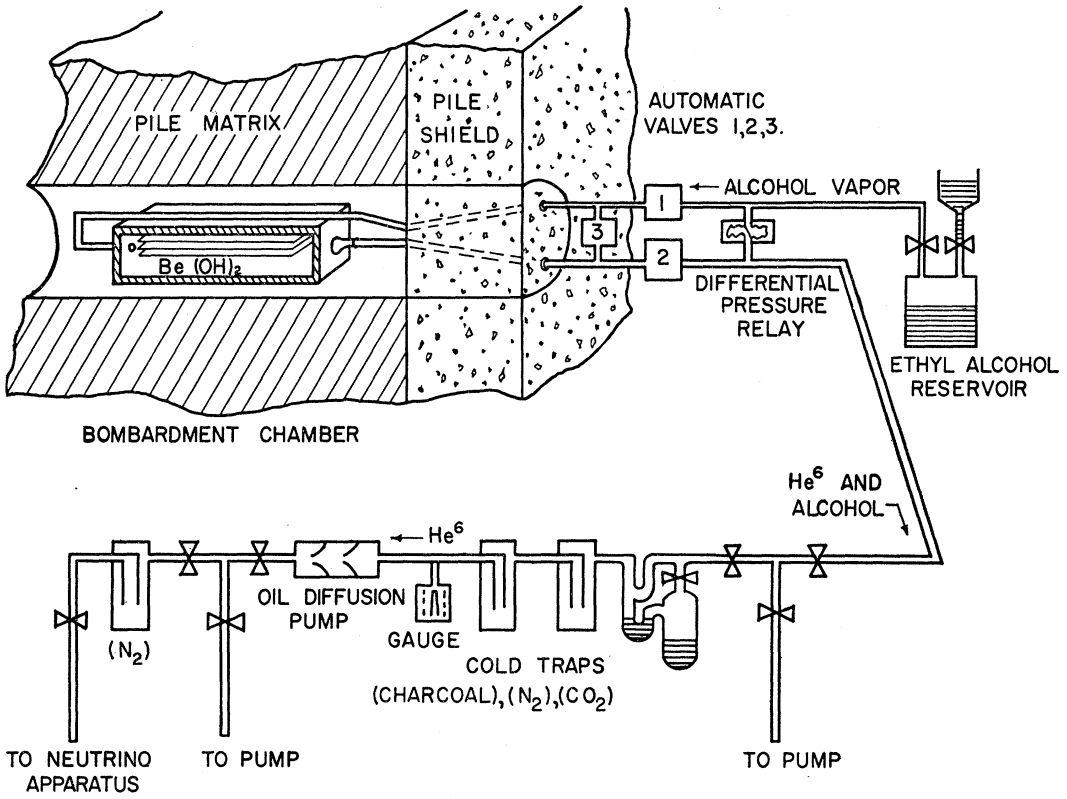

FIG. 1. Schematic diagram of the bombardment chamber and pumping system used to generate He^6 for the angular correlation experiment. The gas is flushed from the chamber, which is located in a position of high neutron flux near the center of the reactor, with ethyl alcohol vapor. The differential pressure relay is a safety feature which automatically isolates the bombardment chamber in case of an accidental break in the pumping system.

maximum energy of the recoil ion is about 1405 ev, one of the highest known for allowed beta-emitters.

The interaction for the He^6-Li^6 transition is expected to be dominated by either the tensor or the axial vector invariant. From the observed energy spectra of allowed beta emitters, Davidson and Peaslee[10] and also Mahmoud and Konopinski[11] have independently determined the magnitude of the Fierz interference term which results from an admixture of these two invariants. Their results set an upper limit of about 4 percent for the (T,A) mixing; and it seems probable that one of the invariants is absent altogether. The Gamow-Teller interaction in the beta-decay Hamiltonian, therefore, can be uniquely identified from the observed e-ν angular correlation of He^6. Preliminary results of this experiment identifying the invariant have been reported.[12] The angular correlation is determined by measuring the coincidence rate between electrons and recoil nuclei as a function of the angle between the particles and also of the energy of the electron. A defined source of the beta-active gas is an essential feature of the experiment. The results, when compared with curves predicted from the Gamow-Teller invariants, have been consistently in good agreement with the tensor curves calculated from the e-ν angular correlation

$$[1+\tfrac{1}{3}(p/W)\cos\phi].$$

II. PRODUCTION OF He^6

The beta-active He^6 was produced according to the reaction $Be^9(n,\alpha)He^6$ by bombarding 250 g of $Be(OH)_2$ powder in the Brookhaven reactor. The powder was specially prepared in a highly emanating form by the method of Sommers and Sherr.[13] The surface area of the powder was approximately 200 square meters per gram, as measured by the Brunauer, Emmett, Teller method of low-temperature absorption of nitrogen. It was noted that the hydroxide produced fifteen times more available He^6 than the equivalent weight of 300-mesh powdered beryllium metal.

The gas pumping system is shown schematically in Fig. 1. $Be(OH)_2$ powder was spread loosely in trays which were stacked in a vacuum-tight aluminum bombardment chamber. The chamber was then placed in an experimental hole at a position near the center of

[10] J. P. Davidson and D. C. Peaslee, Phys. Rev. **91**, 1232 (1953); **92**, 1584 (1953).
[11] H. M. Mahmoud and E. J. Konopinski, Phys. Rev. **88**, 1266 (1952).
[12] B. M. Rustad and S. L. Ruby, Phys. Rev. **89**, 880 (1953).
[13] H. R. Sommers and R. Sherr, Phys. Rev. **69**, 21 (1946).

the reactor. Ethyl alcohol vapor, from a reservoir outside the reactor, was used to sweep the He^6 from the bombardment chamber to the source volume. The vapor pressure above the alcohol in the reservoir, which was kept at room temperature, was about 6 cm Hg.

As a high concentration of He^6 was desired at pressures below 1μ, it was necessary to remove the carrier vapor with a series of cold traps and to concentrate the He^6. The dry-ice trap, shown in Fig. 1, condensed the greater part of the vapor as a liquid which was continually drained off. The vapor pressure above the liquid was 5μ. A liquid nitrogen trap condensed the remaining alcohol vapor and reduced the pressure to about 5×10^{-6} mm Hg. An activated charcoal trap was used to absorb any trace activities, other than He^6, that may have been produced in the bombardment chamber by the intense, complex flux of the reactor. The remaining gas was concentrated by a small 7-liter/second oil diffusion pump, and a second liquid nitrogen trap removed the condensable vapors evolved from the pump. The delivery of the system averaged about 8×10^7 He^6 atoms/sec, when the pile was in normal operation.

The purity of the He^6 activity was determined by measuring the half-life of the gas as a function of the beta-ray energy. The gas was trapped in a small auxiliary source volume by toggle valves which could be tripped in unison by a solonoid. The radiation passing through a 3-mg/cm² mica window was examined with a stilbene scintillation spectrometer; the data was recorded on a fast tape oscillograph. A typical set of half-life results is shown in Fig. 2 in which the activity of the trapped gas in the beta energy range from 1.0 to 1.4 Mev is plotted as a function of time. The logarithmic decay curve is linear, and the observed half-life of 0.85 ± 0.03 second is in excellent agreement with the value of 0.823 ± 0.013 second reported by Holmes.[14] When the charcoal trap was removed, a trace impurity (0.2 percent) was noticed that was identified by its half-life as N^{16}. This activity was expected from the irradiation of oxygen in the ethyl alcohol vapor and beryllium hydroxide powder by fast neutrons in the reactor. Similar results were obtained for other channels in the energy range from 0.5 to 3.5 Mev. A conventional energy spectrum of the source gas was also measured to determine whether an impurity might be present with a half-life close to that of He^6 but of different end-point energy. Although this measurement is less sensitive than the half-life measurements, the Kurie plot of the spectrum shown in Fig. 3 is linear and does not indicate the presence of such an impurity. It is concluded from these results that the beta activity due to impurities was less than 3 percent of the He^6 activity at any energy above 0.5 Mev.

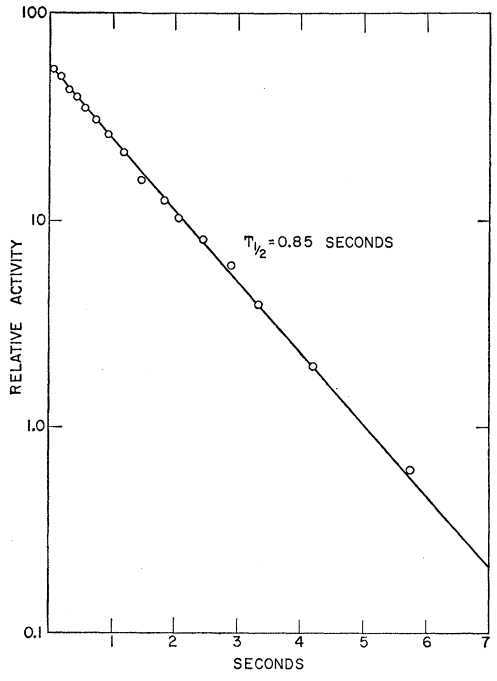

FIG. 2. Radioactive decay curve of the gas delivered from the He^6 generator. The activity was detected with a stilbene scintillation spectrometer adjusted to select beta rays in the energy range from 1.0 to 1.4 Mev.

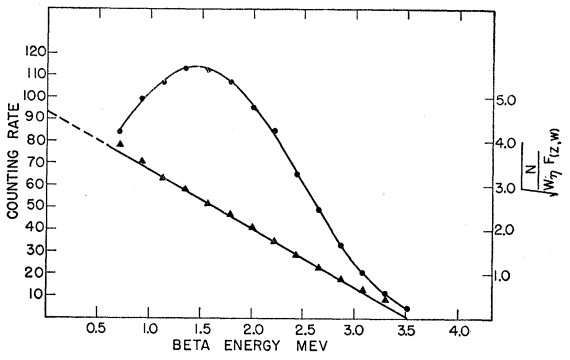

FIG. 3. He^6 beta spectrum measured with the stilbene scintillation spectrometer. The Kurie plot of the spectrum is linear and the end-point is in agreement with the value 3.50 ± 0.05 Mev reported by Wu *et al.* (see reference 8). The slight deviations at the ends of the spectrum are attributable to the resolution width of the spectrometer.

III. DESCRIPTION OF THE APPARATUS

The apparatus used for the electron-recoil nucleus experiment is illustrated by schematic sketches in Figs. 4 and 5. It consists of a defined source of He^6, a collimator and electron multiplier for detecting recoil nuclei, and a stilbene scintillation spectrometer to measure the direction and energy of the beta rays. The decay of a particular nucleus in the source volume is identified by the recording of a coincidence between the scintillation spectrometer and the recoil ion detector.

[14] J. E. R. Holmes, Proc. Phys. Soc. (London) **62**, 293 (1949).

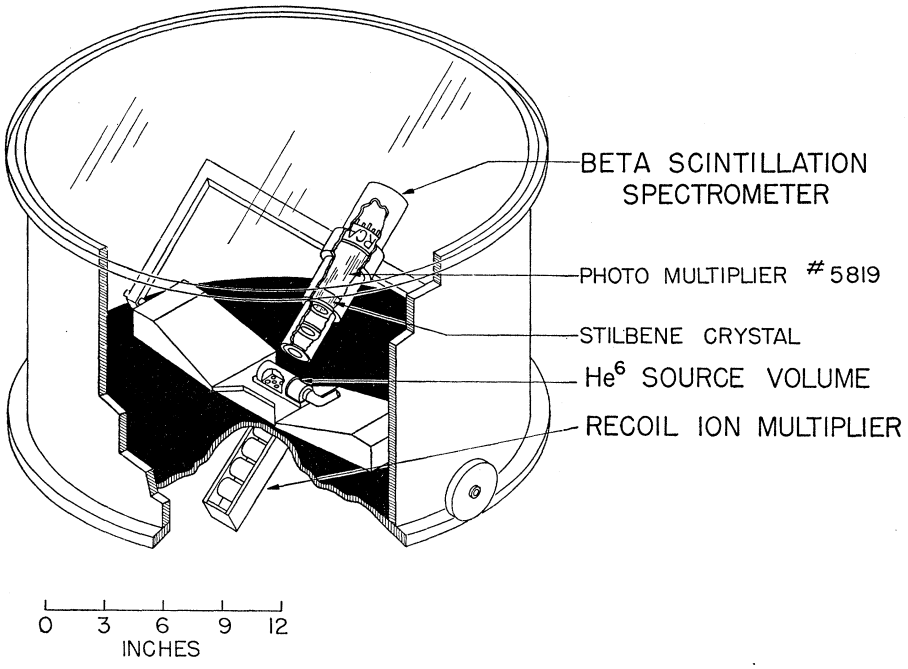

FIG. 4. Schematic sketch of the apparatus used to determine the electron-recoil ion correlation in the decay of He^6. The beta-active source volume and the scintillation spectrometer are located in the common vacuum of the "bell-jar." The pumping diaphragm, which collimates the recoil ions between the source volume and the multiplier, is illustrated in detail in Fig. 5. The vacuum enclosure around the recoil ion multiplier has been omitted for clarity. The differential pumping lines for the diaphragm are shown to the upper left and lower right of the source volume.

A. Beta-Active Source Volume

The He^6 source volume is defined by a 180-microgram/cm^2 aluminum foil and a differential pumping diaphragm. The length of the source is 3.5 cm; and the axis of the semicylindrical surface, which has a radius of 1 cm, is 0.9 cm above the pumping diaphragm. The pumping diaphragm shown in Fig. 5 serves the dual purpose of collimating recoil ions from the source volume and reducing the concentration of He^6 in the region surrounding the recoil ion multiplier. The eight holes in the diaphragm are 0.181 inch in diameter and 0.787 inch in length. Thin aluminum rings, 0.138 inch inside diameter by 0.009 inch thick, in each hole collimate the recoil ions and prevent singly scattered ions from reaching the multiplier. The rings define the direction of the recoil ions to $\pm 10°$. Differential pumping is achieved by evacuating about 90 percent of the gas through the separation at the center of the diaphragm. The pumping diaphragm and the structural parts of the source volume were constructed of polystyrene to minimize the scattering of beta rays. A very thin coating of aluminum was evaporated over the exposed plastic surfaces and grounded to eliminate the collection of static charge which could deflect the recoil ions. A 95 percent transparent tungsten grid is supported on insulators below the pumping diaphragm. This grid was used to repel the recoil ions in auxiliary experiments to test the operation of the apparatus.

The cylindrical "bell jar" surrounding the source volume and the stilbene scintillation spectrometer was evacuated to prevent both the collapse of the very thin foil of the source volume and the possible gas scattering of the beta particles between the source volume and the spectrometer. The pumping diaphragm and the region surrounding the multiplier were each evacuated by a 700-liter/sec oil diffusion pump. A dry ice cold trap before each pump prevented back-diffusing oil vapor from reaching the surfaces of the source volume. The pressure during all data runs was reduced sufficiently so that the mean free path of the recoil ions was large compared to the geometrical dimensions of the apparatus. During a typical data run, the pressure in the "bell jar" was 2×10^{-5} mm Hg, in the multiplier region 3×10^{-6} mm Hg, and in the source volume approximately 0.4 micron. The pressure measurements indicate that the concentration of He^6 near the multiplier was at least one hundred times smaller than in the source volume. Direct counting measurements, with the potential of the repelling grid adjusted to shut off ions from the source volume, resulted in the same conclusion and proved that the particles which were recorded as true coincidences originated in a definite source volume defined by the aluminum foil and the pumping diaphragm.

B. Recoil Ion Multiplier

The recoil ions are detected by a 12-stage Allen-type multiplier. The dynodes of the multiplier were fashioned from Be-Cu alloy and sensitized as suggested by Dare and Rowen[15] by heating the dynodes to 600°C in a hydrogen furnace. The first dynode was held 4000 volts negative with respect to the grounded source volume so that the energy of singly charged ions impinging upon this electrode varied only between 4000 and 5405 ev. The two grids directly below the pumping diaphragm were also grounded during the He^6 data runs to electrostatically shield the recoil-ion collimating apertures in the diaphragm. The output of the multiplier was connected to a linear pulse amplifier of conventional design which had a rise time of 0.18 μsec. Allen reports that the efficiency *vs* energy curve for a Be-Cu multiplier reaches a plateau of about 90 percent efficiency for Li^+ ions in this energy range.[16] To verify this characteristic for the particular multiplier used in the He^6 experiment, the coincidence rate between electrons and recoil ions was measured for various first dynode potentials in the range between 3000 and 5000 volts. No variation in the true coincidence rate greater than that attributed to statistics was found.

C. Stilbene Scintillation Spectrometer

The beta-ray scintillation detector shown in Fig. 4 consists of a collimator to define a beam of electrons, a clear stilbene crystal 4.5 cm in diameter by 1.6 cm thick, and a selected RCA 5819 photomultiplier. The

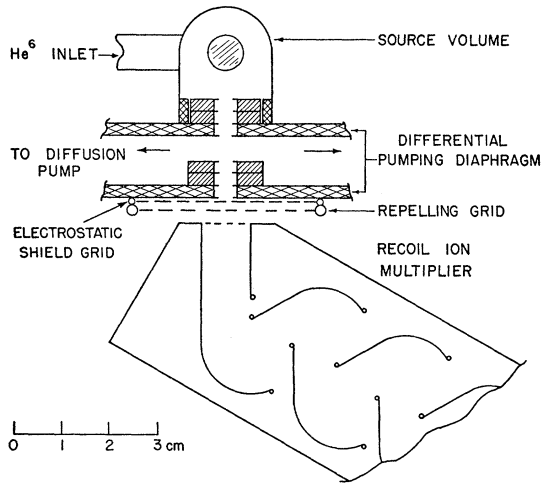

FIG. 5. Schematic cross section of the source volume and the differential pumping diaphragm. Gas from the He^6 generator enters the source volume at the end of the chamber. A collimated beam of Li^+ ions from the decay of He^6 in the source volume is accelerated through a potential difference of 4000 volts between the grounded "repelling" grid and the parallel grid covering the entrance to the multiplier. The recoil ion multiplier is connected in coincidence with the beta scintillation detector shown in Fig. 4.

[15] J. A. Dare and W. H. Rowen, Oak Ridge National Laboratory Technical Report No. 6 (unpublished).

[16] J. S. Allen, Phys. Rev. **75**, 570 (1949).

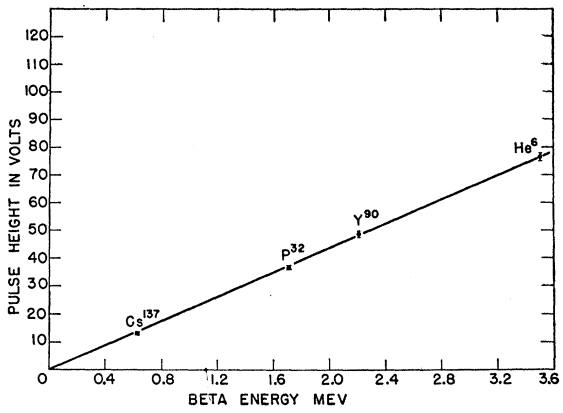

FIG. 6. Pulse height *vs* beta-ray energy calibration for the stilbene scintillation spectrometer.

detector is surrounded by an iron shell which acts as a shield against scattered beta radiation. The entire detector unit, which is enclosed by an iron "bell jar," is clamped to a "U" shaped frame that pivots about the axis of the source volume. The frame is connected to a gear drive operated from outside the vacuum system so that the beta-ray detector may be positioned at angles between 95° and 180° with respect to the recoil ion beam without breaking the vacuum within the "bell jar." The collimator consists of three brass rings which have an inside diameter of 4 cm. The surfaces of the collimator exposed to radiation from the source volume are covered with a $\frac{1}{4}$-in. layer of polystyrene to minimize the scattering and the bremsstrahlung of the incident beta rays. The collimator defines the direction of the beta rays to $\pm 11\frac{1}{2}°$.

The stilbene crystal is covered with 180-microgram/cm² aluminum foil and mounted in a Lucite light-piper which is cemented to the phototube. The foil served as a reflector and also prevented the sublimation of the stilbene crystal into the surrounding vacuum. The output of the phototube is connected to a preamplifier unit mounted on the end of the iron shield. The pulse from the preamplifier is clipped by a shorted delay line to produce an approximately rectangular pulse, one μsec in width, and is amplified with a linear amplifier of the same type used for the recoil ion detector. The energy distribution of the beta rays striking the stilbene crystal was measured with a single-channel pulse-height analyzer.

The energy response and the resolution of the scintillation spectrometer were determined in order to compare the observed coincidence rate between the recoil ion multiplier and the spectrometer with theoretical predictions for the He^6 experiment. Bell[17] and others have reported that the output pulse distribution of a stilbene scintillation detector for monoenergetic electrons is approximately a Gaussian function. The central value of the distribution is proportional to the

[17] P. R. Bell, Phys. Rev. **73**, 1405 (1948).

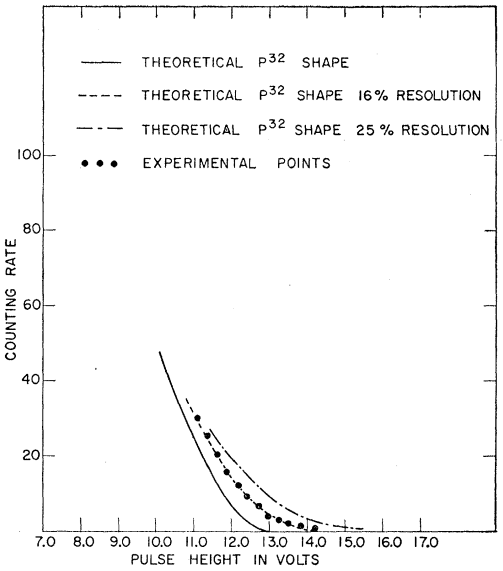

FIG. 7. Comparison of the observed high-energy portion of the P^{32} spectrum with the theoretical shapes calculated for various resolution widths of the scintillation spectrometer. The form of the resolution function is given in Eq. (3).

electron energy and the full width at half maximum varies as the square root of the energy. The energy response of the spectrometer was calibrated with 624-kev internal conversion electrons from Cs^{137} and the Kurie-plot end points of the beta spectra of He^6, P^{32}, and Y^{90}. The results given in Fig. 6 show that the average pulse height of the spectrometer is proportional to the beta-ray energy. The full width at half maximum of the spectrometer pulse distribution for the 624-kev internal conversion electrons of Cs^{137} was 166 kev.

The variation of the resolution with energy was more difficult to determine because monoenergetic beta-ray sources of several Mev energy were not available. The measured shape of a beta spectrum beyond the actual end point, however, is dependent upon the resolution of the spectrometer. The beta spectrum of P^{32} was measured, and a Kurie plot constructed to calibrate the known 1.73-Mev end point of the spectrum with the pulse height output of the spectrometer. Theoretical spectrum curves were calculated for several different resolution widths and normalized to the experimental data at the midpoint of the spectrum. The best agreement between the theoretical curves and the experimental data, as seen in Fig. 7, occurs for a spectrometer resolution of 16 percent. This result is in good agreement with the prediction, based on the spectrometer resolution for Cs^{137} electrons, that the full width at half maximum varies as $0.21E^{\frac{1}{2}}$, where E is the kinetic energy of the electron measured in Mev.

Careful measurements were also taken of the He^6 spectrum at angles of 100°, 145°, and 180° between the particle detectors to determine if there were any angular discrimination in the apparatus. The Kurie plots of these spectra were found to be almost exactly identical, agreeing within ±1 percent from 0.75 Mev to the maximum beta-ray energy of He^6.

D. Electron-Recoil Ion Coincidence Spectrometer

The amplifier and coincidence circuits for the particle detectors are indicated by block diagram in Fig. 8. The output of each of the detector amplifiers was brought to a calibrated discriminator. A lumped constant delay line, which could be varied between 0 and $\frac{1}{2}$ μsec, was introduced into the beta channel to compensate for the difference in transit time of the pulses in the two channels. This delay line was also used to retard the pulse from the scintillation detector by an additional 0.08 μsec, which is slightly less than the shortest time-of-flight of the most energetic recoil nuclei between the source volume and the multiplier. The total number of pulses in each detector channel was recorded by a fast scaler and register.

The decay of a nucleus in the source volume was detected by connecting the detector channels in coincidence at Mixer No. 1. The beta pulse actuated a modified Schmidt trigger and delay line combination which produced a rectangular pulse of constant amplitude that could be varied in width from 0.1 to 1.28 μsec. A triangular pulse, with a full width at half maximum of 0.05 μsec, was produced by a blocking oscillator when triggered by the discriminator in the recoil ion channel. Coincidences between these shaped pulses were detected in Mixer No. 1 and recorded with a scaler and register. During the He^6 experiment, the resolving time of the coincidence circuit was set for 1.07 μsec as measured by recording accidental coincidences between the two particle detectors. This time interval is sufficiently long to detect recoil nuclei with energies down to about 140 ev. The number of true coincidences resulting from the decay of single nuclei was obtained by subtracting the accidental coincidences from the total number recorded. The number of accidental coincidences (A) in any time interval was calculated from the simple relation $A=\tau n_M n_B/T$, where τ is the resolving time of the circuit and n_M and n_B are the total number of pulses recorded during time T by the recoil ion multiplier and the beta detector, respectively. This relation is valid if the counting rate in each detection channel is constant; a rate meter and recording oscillograph were connected to the beta-detector channel to insure that there were no appreciable variations in source activity during a run. It is evident that any variation or drift in the value of τ would directly affect the data measured with these circuits. The resolving time was, therefore, determined at frequent intervals during data collection with an accurately calibrated double pulser and was found to be reproducible to ±2 percent, which is significantly smaller than the statistical variation in the He^6 coincidence data.

A pulse-height analyzer is also connected to the output of the beta channel amplifier to select beta rays

of given energy. Coincidences between Mixer No. 1 and the pulse height analyzer were detected by Mixer No. 2 which had a resolving time of 6 μsec. The scaler and register for this second coincidence circuit record the number of recoil ions that are detected in coincidence with electrons of pre-selected energy.

IV. CALCULATION OF EXPECTED RESULTS

The e-ν angular correlations derived from various forms of the beta-decay interaction Hamiltonian are written customarily in terms of the angle ϕ between the electron and neutrino. Since neither the angle nor the correlation can be directly measured, it seemed appropriate to perform a transformation to some new set of variables which are observable. The results of a particular experiment can then be compared immediately with the various predictions. The relativistic energy W of the electron and the angle θ between the recoil nucleus and the electron were chosen for the parameters of this experiment after a study of the theoretical and experimental factors involved. The e-ν angular correlation transforms to $R(W,\theta)$, the probability density that the nucleus recoils at an angle θ with respect to the direction of an electron which was emitted with an energy W. The most important property of $R(W,\theta)$, as may be seen in following figures, is that the shape of this function depends critically upon the particular form assumed for the interaction Hamiltonian. This choice of variables is also favorable because the quantities $R(W,\theta)dWd\theta$, θ and W can be measured by relatively simple experimental techniques.

The probability of an allowed beta-active nucleus emitting a neutrino into a solid angle element $d\omega$ at an angle ϕ with respect to an electron of energy W has been derived by De Groot and Tolhoek[2] on the basis of an arbitrary linear combination of the five invariants. The form of this expression, when specialized for the He^6 transition, becomes

$$P(W,\phi)dWd\omega=pW(W_0-W)^2\left|\int\boldsymbol{\sigma}\right|^2F(Z,W)\times[1+\gamma]\left[1+\alpha\frac{p}{W}\cos\phi\right]dWd\omega, \quad (1)$$

$$\alpha=-\frac{1}{3}\frac{(1-X^2)W}{(1+X^2)W+2X}, \quad \gamma=\frac{2X}{(1+X^2)W}, \quad X=\frac{G_A}{G_T},$$

where G_A and G_T are the mixing coefficients of the A and T invariants in the interaction Hamiltonian $H=(G_AA+G_TT)$, $|\int\boldsymbol{\sigma}|^2$ is the square of the Gamow-Teller matrix element, and $F(Z,W)$ is the Coulomb correction function. It has been shown by Biedenharn and Rose[18] from time-reversal considerations that the coefficients G_A and G_T are real constants. The probability density $R(W,\theta)$ may be obtained from Eq. (1)

[18] L. C. Biedenharn and M. E. Rose, Phys. Rev. **83**, 459 (1951).

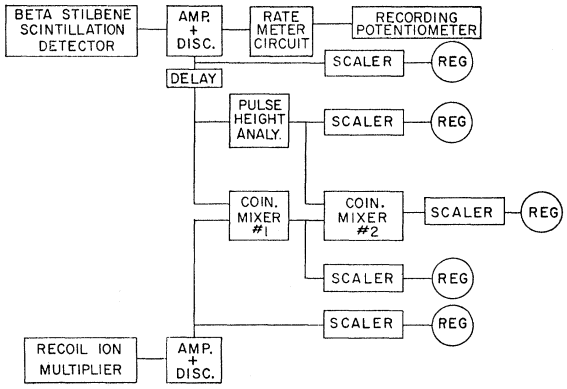

FIG. 8. Block diagram of the electron-recoil ion coincidence spectrometer.

if the conservations of energy and momentum are assumed for the decay products.

In an actual experiment, it is difficult to approximate point sources and detectors, and the expected coincidence rate must be obtained by integrating $R(W,\theta)dWd\Omega$ over the finite solid angles subtended by the detectors, the volume of the source, and the energy resolution of the beta-ray spectrometer and recoil-ion detector. The expected coincidence rate $C(W,\theta)$ has the form

$$C(W,\theta)=\sum_{i=1}^{2}\int\int pW(W_0-W)^2F(Z,W)g_i(W,\theta)\times[1+\gamma][1+\alpha f_i(W,\theta)]T(W,E_1,E_2)T(E_R)dWd\Omega, \quad (2)$$

where

$$f_i(W,\theta)\equiv\cos\phi=-y\sin^2\theta\mp\cos\theta(1-y^2\sin^2\theta)^{\frac{1}{2}},$$
$$y=(W^2-1)^{\frac{1}{2}}/(W_0-W),$$
$$g_i(W,\theta)=(\sin\phi d\phi)/(\sin\theta d\theta),$$

and the summation over i is introduced to indicate that ϕ is a double valued function of θ when y is greater than 1. The factor $g_i(W,\theta)$ expresses the transformation between the solid angle elements $d\omega$ and $d\Omega$.[19] The resolution function of the stilbene scintillation spectrometer is approximated, as was discussed earlier, by the Gaussian curve

$$T(W,E_1,E_2)=\int_{E_1}^{E_2}\frac{1}{[2\pi k(W-1)]^{\frac{1}{2}}}\exp\left(\frac{(W-E)^2}{2k(W-1)}\right)dE. \quad (3)$$

The limits E_1 and E_2 of the integral define the pulse-height-selector channel width, and k is proportional to the square of the full width at half maximum of the pulse-height distribution function of the stilbene beta

[19] A detailed examination of the integrand of Eq. (2) has recently been published by O. Kofoed-Hansen, Kgl. Danske Videnskab. Selskab, Mat.-fys. Medd. **28**, No. 9 (1954) and Reynolds, Biedenharn, and Beard, Oak Ridge National Laboratory Report ORNL-1444 (unpublished).

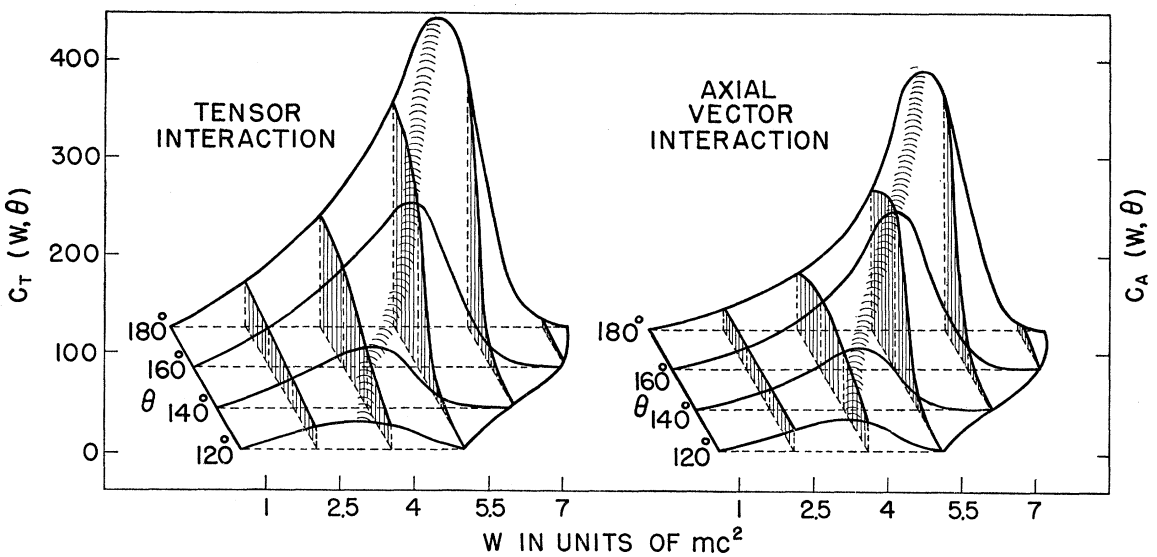

FIG. 9. The coincidence rate functions, $C_T(W,\theta)$ and $C_A(W,\theta)$, predicted from the pure tensor and axial vector invariants, respectively, represented as three-dimensional surfaces.

detector. The resolution function $T(E_R)$ of the recoil ion detector may be approximated by a suitable step function with parameters chosen to correspond to the resolving time of the coincidence circuit and the time-of-flight spectrum of the recoil ions.

The integration of $C(W,\theta)$ was performed numerically over appropriate limits corresponding to the geometry and energy resolution of the apparatus used for the He^6 experiments. The form of $C(W,\theta)$ is dependent upon the e-ν angular correlation coefficient α which in turn is a function of the mixing coefficients of the invariants and the energy of the electron. The angular correlation coefficient has the values $+1$, $+\frac{1}{3}$, $-\frac{1}{3}$, and -1 for pure V, T, A, and S invariants, respectively. Curves corresponding to these choices are presented for reference in the following section.

V. EXPERIMENTAL RESULTS

The coincidence rate between the detectors of the electrons and recoil nuclei was measured as a function of the angle (θ) between the particles and the beta-ray energy (W). Since the interaction Hamiltonian for the He^6—Li^6 transition is expected to be dominated by either the tensor (T) or the axial vector (A) invariant, the functions $C_T(W,\theta)$ and $C_A(W,\theta)$ were calculated assuming a pulse-height-selector channel width of 1 mc^2 to determine the experimental parameters which would provide the most sensitive test to distinguish between these invariants. In Fig. 9, the two expressions are represented by three-dimensional surfaces. The projection is chosen to make both surfaces completely visible even though this tended to minimize the difference between the two figures. Both surfaces are peaked in the "forward" direction at approximately $W=6.5\ mc^2$, $\theta=180°$. The shape and height of the surfaces differ considerably, as may be observed from the cross sections outlined at equal intervals along the coordinates. The absolute difference in height is largest at $\theta=180°$; the shapes of the surfaces vary to the greatest extent along cross sections taken at constant energy in the range from about 2.5 to 5.5 mc^2. In view of the difficulty in eliminating every possible source of consistent error in an absolute determination of the electron-recoil nucleus correlation, it was decided instead to measure a family of coincidence rate curves relative to an arbitrary source strength and to normalize the resulting data to the predicted curves.

A. Electron-Recoil Ion Angular Correlation

In Fig. 10, the observed coincidence rate is plotted at angular intervals of 10° with the spectrometer channel width set to detect beta rays in the range from 2.5 to 4.0 mc^2. The coincidence rate corresponding to these low-energy beta particles was small; and the channel width was purposely made broad in order to collect data in reasonable time. The experimental points represent the weighted average of ten individual measurements over the angular range. The error bars indicate the statistical variation in the weighted data. As the time required to collect these results covered many days, each run over the angular range was taken in a short period with relatively poor statistics so that the effect of any gradual time variation in the performance of the apparatus would be minimized. The He^6 source was monitored with the recoil-ion detector, and the data normalized to a given source activity to adjust for the variations in source strength caused by occasional small changes in the power level of the pile.

Curves of the expression $C(W,\theta)$ calculated for the channel width 2.5 to 4.0 mc^2 on the bases of the T, A,

V, and S invariants are presented for comparison with the experimental data. The calculated curves have been normalized to the data at the cross-over point $\theta=128°$, where all four pure invariants predict the same coincidence rate. To decrease the statistical error of the normalization coefficient, the calculation was averaged over the three points nearest to the cross-over by determining the ratio of the integrated area under the theoretical curves to that of the data at 120°, 125°, and 130°. The observed coincidence rate, when compared with the various predictions, agrees within statistics with the tensor curve and cannot be made to fit the other invariants.

The other members of this family of curves are shown in Figs. 11 and 12. The observed coincidence rate was measured for the beta-ray energy ranges, 4.5 to 5.5 mc^2 and 5.5 to 7.5 mc^2, respectively. The corresponding predicted curves become progressively more similar in shape and the cross-over occurs at increasingly higher angles (150° and 163°, respectively) as the energy selected in the beta-ray spectrometer is increased. The curves calculated for the channel width, 4.5 to 5.5 mc^2 are sufficiently different to provide another good test for the interaction. Three measurements over the angular range were weighted and averaged. The areas from 145° to 155° under the predicted curves and the data were determined in order to calculate the normalization coefficient at the cross-over point. In Fig. 11 it may be seen that the coincidence rate is again in agreement with just the tensor curve. Since the predicted curves for the energy range 5.5 to 7.5 mc^2 are nearly alike in shape and coincidence rate, no attempt was made to collect data with the statistical accuracy required for a positive identification of the He^6 interaction. The few experimental points, however, do tend to favor the tensor invariant.

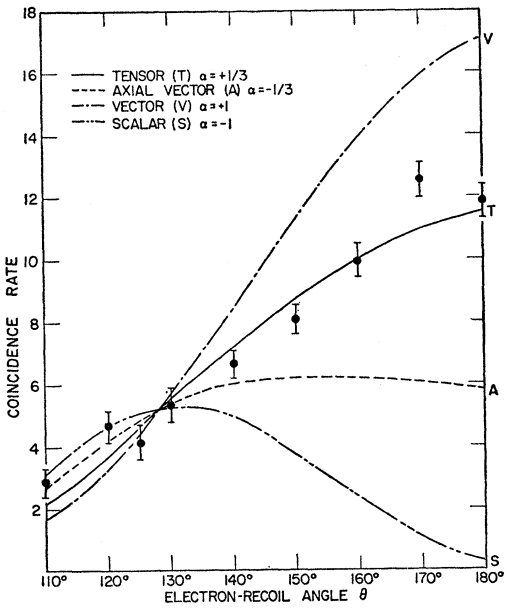

FIG. 10. The first electron-recoil ion, angular correlation measurement. The coincidence rate was measured as a function of the angle θ between the particles with the scintillation spectrometer adjusted to detect beta rays in the energy range from 2.5 to 4.0 mc^2. The curves, which were calculated from Eq. (2) on the basis of the T, A, V, and S invariants, are normalized to the experimental data at the common "cross-over" point.

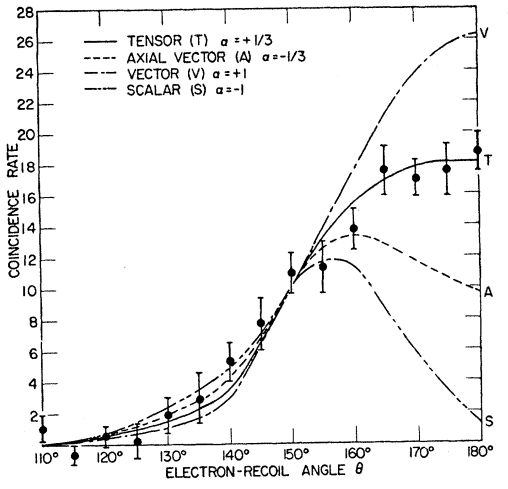

FIG. 11. The second electron-recoil ion, angular correlation measurement. Only those coincidences for beta rays with energy between 4.5 and 5.5 mc^2 are recorded. The predicted curves are normalized to the data at 150°. Chance coincidences have been subtracted from the total number which were detected, and the appearance of data at negative rates is caused by the statistical fluctuations in these measurements.

The data of Fig. 12 are of importance in that they provide a sensitive test for the effect of scattering of electrons and recoil ions in the apparatus used for the experiment. The predicted coincidence rates for all four invariants approach zero at 140° in Fig. 12 and 110° in Fig. 11. These angles, which are often referred to as the "momentum cutoff," can also be derived from a classical momentum diagram of the He^6 decay products. For beta rays of momentum (p) and neutrinos of corresponding momentum (q), the limiting cut-off angle, which occurs only for $p>q$ is given by $\sin\theta_c=+q/p$; and coincidences at smaller angles are forbidden by the conservation of momentum. The recoil nucleus is directed into the opposite hemisphere from the electron; and the cut-off angle approaches 180° as the electron carries away an increasingly greater proportion of the energy available to the transition. Any high-angle scattering of recoil ions or beta rays of the selected energy from the walls of the source volume and the collimators should produce coincidences at angles smaller than the momentum cutoff. From Figs. 11 and 12, it may be seen that these "scattered" events are negligible since the measured coincidence rates after the subtraction of accidentals are zero below the predicted cut-off angles.

B. Electron-Recoil Ion Coincidence Spectrum

The coincidence rate between the electrons and recoil nuclei was also measured as a function of the beta-ray

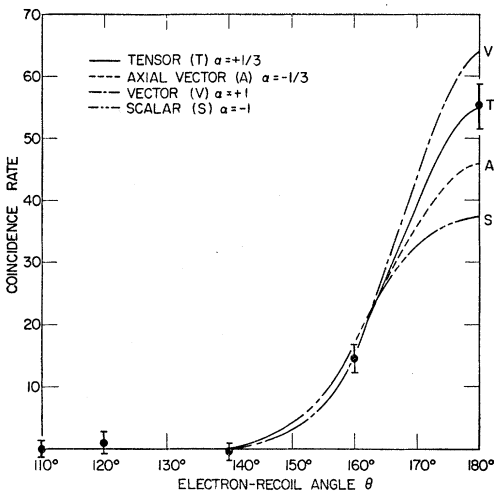

FIG. 12. The third electron-recoil ion, angular correlation measurement. The energy range selected for the beta rays is 5.5 to 7.5 mc^2. The measured coincidence rates are zero at angles smaller than about 140° in agreement with the predicted curves and the classical value for the "momentum cutoff."

energy with the angle between the detectors held fixed. This measurement was performed to obtain data for the identification of the electron-neutrino correlation which would be independent of any possible angular discrimination in the apparatus, even though the measurements of the He^6 energy spectrum *vs* angular displacement did not reveal such discrimination. The coincidence data were taken at the angle $\theta=180°$ with an energy channel width of $1\ mc^2$. Four separate measurements were taken over the He^6 energy spectrum and averaged.

The comparison of the T and A cross sections at $\theta=180°$ in Fig. 9 shows that the curves do not cross to provide the obvious normalization point found in the angular correlation predictions. An alternate method was used, therefore, in which the integrated area under the predicted curves was normalized to the total number of coincidences that were recorded over the He^6 spectrum. It should be noted that this procedure preserves the shape but not the proportional magnitude between the T and A curves. The results of this experiment are presented in Fig. 13. The coincidence rate data lie on the tensor curve; and the consistency of these measurements with the angular correlation determinations support the conclusion that the beta-decay interaction for the He^6-Li^6 transition is dominated by the tensor invariant.

VI. ANGULAR CORRELATION COEFFICIENT

Although agreement is found between the predicted tensor curves and the measured electron-recoil nucleus coincidence rates, a determination of the angular correlation coefficient α is necessary in order that the results of this experiment may be quantitatively compared with the analysis of beta spectra for the existence of the Fierz interference term, $2X/(1+X^2)W$. From Eq. (2), it may be seen that the shape of the coincidence rate curve, $C_0(W,\theta)$ *vs* θ for constant W, depends upon factors involving W and θ and also upon the magnitude of the coefficient $\alpha=\frac{1}{3}(1-X^2)W/[(1+X^2)W+2X]$ which precedes the angular term $f(W,\theta)$. A detailed examination of the data was carried out in which an observed α_0 was determined for every experimental point, other than these used for normalization, from the expression

$$\alpha_0=\frac{\left(nC_0(W,\theta)-\int\int P_F dW d\Omega\right)}{\int\int P_F \frac{p}{W} f(W,\theta) dW d\Omega}, \tag{4}$$

where the measured coincidence rate is

$$C_0(W,\theta)=k\int\int P_F\left[1+\alpha\frac{p}{W}f(W,\theta)\right]dW d\Omega, \tag{5}$$

the normalization coefficient is

$$n=\frac{\int_c\int P_F dW d\Omega}{\left\{k\int_c\int P_F\left[1+\alpha\frac{p}{W}f(W,\theta)\right]dW d\Omega\right\}}, \tag{6}$$

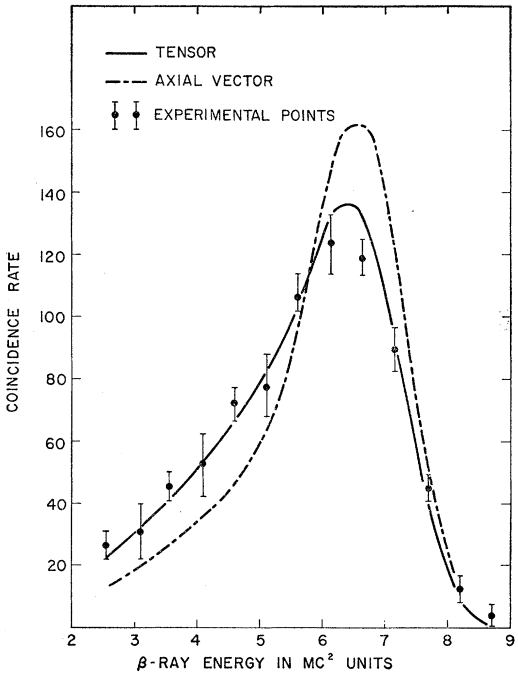

FIG. 13. The electron-recoil ion coincidence spectrum. The coincidence rate was measured as a function of the beta-ray energy with the angle θ between the detectors held fixed at 180°. The channel width of the scintillation spectrometer was $1\ mc^2$. The curves predicted from the T and A invariants are normalized to the total number of coincidences recorded over the spectrum.

and

$$P_F=(G_A^2+G_T^2)(1+\gamma)pW(W_0-W)^2F(Z,W)$$
$$\times\left|\int\sigma\right|^2 g(W,\theta)T(W,E_1,E_2)T(E_R). \quad (7)$$

The proportionality constant k, the ratio between the actual He^6 source intensity and the unit source strength assumed in numerical integration, indicates the terms which are experimentally measured. The subscript (c) denotes the evaluation of the respective integral at the cross-over point which was chosen for normalization. The remaining notation is the same as defined in Sec. IV. The summation over the index (i) has been omitted for simplicity and should be understood.

For the experimental conditions of the data given in Figs. 10, 11, and 12, the expression for α_0 reduces identically to $\alpha=\frac{1}{3}(1-X^2)W/[(1+X^2)W+2X]$ except for the indeterminate (0/0) which occurs at the normalization point. The reduction follows when it is observed that the energy limits, E_1 and E_2, were held fixed for each of the curves measured and that the magnitude of α is essentially constant between these energy limits if (X) is taken to be of the order of less than 0.1 or greater than 10.

From the coincidence rate data for the β-ray energy range 2.5 to 4.0 mc^2, six individual determinations of α_0 were calculated. The weighted average of these values is $\alpha_{1.25}=0.36\pm0.11$, where the precision is calculated from the statistical variations of the measured coincidence rates and the mean beta energy in Mev is indicated by the subscript. For the energy range 4.5 to 5.5 mc^2, a similar determination yielded $\alpha_{2.0}=0.31\pm0.14$ as the weighted average of twelve different values. These results may be compared with the coefficients for the pure invariants $\alpha_T=+\frac{1}{3}$ and $\alpha_A=-\frac{1}{3}$.

In Fig. 14, the analytic form of the coefficient α is plotted as a function of $X=G_A/G_T$ for the mean β energy, 2.0 Mev. It is noted by the authors that this function has been independently derived for the special case of point sources and detectors by Kofoed-Hansen and Winther.[20] Their paper also points out that X is a double-valued function of α. It is interesting that the value of α as observed in this type of experiment could exceed $\frac{1}{3}$ in absolute magnitude even though only linear mixtures of the T and A invariants are considered (e.g., the value of α approaches unity for the mixing ratio $X=-\frac{1}{2}$ and $W\sim1$). The curve for the mean beta energy 1.25 Mev is very nearly the same as that shown in the above figure, and a separate graph has not been included. The two determinations of α_0 are shown next to the peak of the plotted curve.

[20] O. Kofoed-Hansen and Aage Winther, Phys. Rev. **89**, 526 (1953).

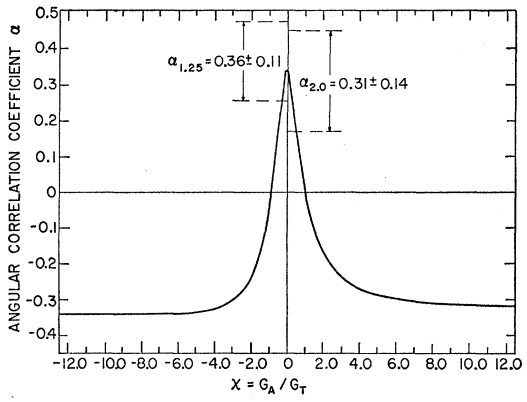

FIG. 14. The angular correlation coefficient, $\alpha=\frac{1}{3}(1-X^2)W/[(1+X^2)W+2X]$, plotted as a function of $X=G_A/G_T$. The coefficients, α_0, determined from the electron-recoil ion correlation of He^6, are shown next to the peak of the curve so that the corresponding range in X [i.e., of (T,A) mixtures] may be observed.

VII. DISCUSSION OF RESULTS

The most recent value appearing in the literature for (T,A) mixtures[10] may be expressed by the alternate limits, $G_A/G_T\leqslant0.04$ or $G_A/G_T\geqslant25$, since the dominant invariant cannot be determined from the magnitude of the Fierz interference term alone. From an enlargement of Fig. 14, the ratio $X=G_A/G_T$ corresponding to the observed e-ν angular correlation coefficient for He^6 is estimated to be within the range, $-0.5<G_A/G_T<+0.3$. This result clearly identifies the mixture of Gamow-Teller invariants as $G_A\leqslant0.04G_T$, where G_A should not be taken as significantly different from zero. The corresponding limits for the e-ν angular correlation coefficient of He^6 are $+0.325<\alpha<+0.340$.

Since He^6 decay obeys only the Gamow-Teller selection rules, other transitions must be examined to obtain further information on the invariants.[21] The complete beta-decay interaction is generally assumed to be a linear combination of one or more of the five pure invariants[22]; and altogether, there are thirty-one possible combinations. However, empirical evidence based upon the precise determination and analysis of a large number of beta spectra greatly restricts the number of combinations. The comparative ft values of the superallowed transitions indicate that the beta-decay interaction contains both the Fermi (S and V) and Gamow-Teller (T and A) types of invariants in approximately equal proportions,[23] and the magnitudes of the Fierz

[21] *Note added in proof.*—Recent measurements of the e-ν angular correlation of Ne^{19} reported by Maxon, Allen, and Jentschke [Bull. Am. Phys. Soc. **29**, No. 7, 15 (1954)] and by W. P. Alford and D. R. Hamilton [Phys. Rev. **94**, 779 (1954)] indicate that the beta-decay interaction contains the scalar invariant (S) and that the vector (V) contribution is small or zero.

[22] H. A. Bethe and R. F. Bacher, Revs. Modern Phys. **8**, 82 (1936).

[23] O. Kofoed-Hansen and A. Winther, Phys. Rev. **86**, 428 (1952); G. Trigg, Phys. Rev. **86**, 506 (1952); J. M. Blatt, Phys. Rev. **89**, 83 (1953); B. R. Bouchez and R. Mataf, Compt. rend. **234**, 86 (1952).

interference terms derived from the observed shape of allowed spectra, as has been discussed, provide convincing evidence against the combinations (T,A) and (S,V). These two important observations reduce the possible combinations to (S,T), (S,A), (V,T), and (V,A) with the inclusion of P undecided. Similar arguments, though less certain, against the combinations (S,A) and (V,T) have been advanced by Mahmoud and Konopinski,[11] which are based on the observed statistical shape of first forbidden spectra. The present identification of T as the Gamow-Teller invariant further narrows the possibilities for the beta-decay interaction to a form containing either the (S,T) or the less probable (V,T) combination of invariants.

The authors wish to express their appreciation to Professor W. W. Havens, Jr. and Professor C. S. Wu for their many helpful suggestions and stimulating discussions during the course of this work. It is a pleasure to acknowledge the cordial hospitality of the Brookhaven National Laboratory. In particular, we wish to thank Dr. M. Fox and the Reactor Group for assistance in making bombardments.

PHYSICAL REVIEW VOLUME 97, NUMBER 4 FEBRUARY 15, 1955

Simple Model of the Li^6 Nucleus and the $Li^6(n,t)He^4$ Reaction

J. DĄBROWSKI AND J. SAWICKI
Institute of Theoretical Physics, University of Warsaw, Warsaw, Poland
(Received November 1, 1954)

A model of the Li^6 nucleus consisting of an alpha particle plus a deuteron is used to calculate angular distributions of the $Li^6(n,t)He^4$ reaction for several neutron energies under the assumption that it is a pickup process. The shapes of the calculated angular distributions are similar to those of the experimental data; however, there is a lack of agreement between experiment and theory at large angles that is ascribed to compound nucleus formation.

RECENTLY[1,2] a simple two-body model for the Li^6 nucleus has been used to discuss the photodisintegration $Li^6(\gamma,d)He^4$. This "α particle+deuteron" model is supported by the following evidence.

(1) The (γ,d) threshold energy is very low (1.477 Mev), whereas the average binding energy per nucleon is ~5.3 Mev and the threshold energies for (γ,n) and (γ,p) are, respectively, ~5.8 and 4.7 Mev; the energy for the disintegration $Li^6+\gamma=3H^2(=H^3+He^3)$ is ~25 Mev (~16 Mev).

(2) The spin $I=1$ is the same as that of the deuteron, while the α particle has spin zero.

(3) The magnetic moment $\mu\cong$the magnetic moment of the deuteron. [(2) and (3) suggest that the "$\alpha+d$" system is in an S-state.]

(4) The present model satisfactorily explained the results of Glenn[3] and of Jensen and Gis[2] for the (γ,d) reaction.[1]

(5) It is also consistent with the results of Lauritsen, Huus, and Nilsson[4] concerning α-d scattering.

It seems to be important to investigate the pickup reaction $Li^6(n,t)He^4$ with the help of this model and to compare the theoretical results with the experimental data of Frye[5] and of Weddell and Roberts.[6]

On applying the Born approximation as done previously,[7] we get the differential cross section in the c.m. system:

$$d\sigma/d\Omega=\left(\frac{1}{2\pi\hbar^2}\right)^2 M_t^* M_0^* \left(\frac{k_t}{k_0}\right)\left(\frac{1}{2\cdot 3}\right) \sum_{\mu_0,\mu_d,\mu_t} |\langle \chi_\alpha \chi_t \exp[i\mathbf{k}_t\cdot(\mathbf{r}-\mathbf{s}/3)]|V_{n_0 d}|\psi_0\rangle|^2, \quad (1)$$

where $M_t^*=(12/7)M$ and $M_0^*=(6/7)M$ are respectively the reduced masses of the triton and the incident neutron (M being the nucleon mass); $\mathbf{k}_t$ and $\mathbf{k}_0$ are their respective momenta in the c.m. system; μ_0, μ_d, μ_t are the neutron, deuteron, and triton magnetic quantum numbers; $\chi_\alpha=\chi_\alpha(\xi)$ is the internal wave function

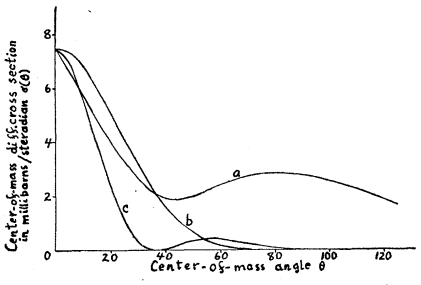

FIG. 1. Angular distribution of tritons from $Li^6(n,t)He^4$ for 14-Mev neutrons. a denotes the experimental curve; b and c—the theoretical curves for $R_0=4\times10^{-13}$ cm and 6×10^{-13} cm, respectively. The theoretical curves represent relative values.

[1] I. S. Waszakidze and G. A. Czilaszwili, J. Phys. (U.S.S.R.) **26**, 254 (1954).
[2] P. Jensen and K. Gis, Z. Naturforsch. **8a**, 137 (1953).
[3] H. B. Glenn, Phys. Rev. **88**, 418 (1952).
[4] Lauritsen, Huus, and Nilsson, Phys. Rev. **92**, 1501 (1953).
[5] Glenn M. Frye, Jr., Phys. Rev. **93**, 1086 (1954).
[6] J. B. Weddell and J. H. Roberts. Phys.. Rev. **95**, 117 (1954).
[7] J. Dabrowski and J. Sawicki, Nuovo cimento **12**, 293 (1954).